The EMBO Journal (2011) 30, 17–31 | © 2011 European Molecular Biology Organization | All Rights Reserved 0261-4189/11
www.embojournal.org

THE EMBO JOURNAL

Interaction of calmodulin with Sec61α limits Ca^{2+} leakage from the endoplasmic reticulum

Frank Erdmann[1,5,6], Nico Schäuble[2,5], Sven Lang[2], Martin Jung[2], Alf Honigmann[1], Mazen Ahmad[3], Johanna Dudek[2], Julia Benedix[2], Anke Harsman[1], Annika Kopp[1], Volkhard Helms[3], Adolfo Cavalié[4,*], Richard Wagner[1,*] and Richard Zimmermann[2,*]

[1]Biophysics, Osnabrück University, Osnabrück, Germany, [2]Medical Biochemistry and Molecular Biology, Saarland University, Homburg, Germany, [3]Computational Biology, Saarland University, Saarbrücken, Germany and [4]Experimental and Clinical Pharmacology and Toxicology, Saarland University, Homburg, Germany

In eukaryotes, protein transport into the endoplasmic reticulum (ER) is facilitated by a protein-conducting channel, the Sec61 complex. The presence of large, water-filled pores with uncontrolled ion permeability, as formed by Sec61 complexes in the ER membrane, would seriously interfere with the regulated release of calcium from the ER lumen into the cytosol, an essential mechanism for intracellular signalling. We identified a calmodulin (CaM)-binding motif in the cytosolic N-terminus of mammalian Sec61α that bound CaM but not Ca^{2+}-free apocalmodulin with nanomolar affinity and sequence specificity. In single-channel measurements, CaM potently mediated Sec61-channel closure in Ca^{2+}-dependent manner. At the cellular level, two different CaM antagonists stimulated calcium release from the ER through Sec61 channels. However, protein transport into microsomes was not modulated by Ca^{2+}-CaM. Molecular modelling of the ribosome/Sec61/CaM complexes supports the view that simultaneous ribosome and CaM binding to the Sec61 complex may be possible. Overall, CaM is involved in limiting Ca^{2+} leakage from the ER.

The EMBO Journal (2011) **30,** 17–31. doi:10.1038/emboj.2010.284; Published online 23 November 2010
Subject Categories: membranes & transport; signal transduction
Keywords: calmodulin; endoplasmic reticulum; ER calcium leakage; IQ motif; Sec61 complex

*Corresponding authors. A Cavalié, Experimental and Clinical Pharmacology and Toxicology, Saarland University, Homburg 66421, Germany. Tel.: +496 841 162 6151; Fax: +496 841 162 6402; E-mail: adolfo.cavalie@uks.eu or R Wagner, Biophysics, Osnabrück University, Osnabrück 49076, Germany. Tel.: +495 419 692 851; Fax: +495 419 692 243; E-mail: wagner@uos.de or R Zimmermann, Medical Biochemistry and Molecular Biology, Saarland University, Building 44, Homburg 66421, Germany. Tel.: +496 841 162 6510; Fax: +496 841 162 6288; E-mail: bcrzim@uks.eu
[5]These authors contributed equally to this work
[6]Present address: Physiologie I, Universität Münster, Münster 48149, Germany

Received: 25 May 2010; accepted: 22 October 2010; published online: 23 November 2010

Introduction

In eukaryotes, the endoplasmic reticulum (ER) has central roles in the synthesis, folding, and sorting of proteins as well as in acting as a dynamic calcium reservoir, which is essential for cellular calcium signalling, a process tightly controlled by electrical and chemical stimuli (Berridge, 2002). How are these key processes coordinated to maintain the functional integrity of the ER?

The products of almost a third of eukaryotic genes are integrated into the membrane or transported to the lumen of the ER (Blobel and Dobberstein, 1975), facilitated by a protein translocase with Sec61α, Sec61β, and Sec61γ as core components (Görlich and Rapoport, 1993; Hartmann *et al*, 1994). Channel pore diameters have been shown to range from 5–8 Å for the closed crystal structure of the archaean ortholog (van den Berg *et al*, 2004) to 26–60 Å for the mammalian Sec61 complex as deduced from fluorescence quenching (Hamman *et al*, 1997) and electrophysiological experiments (Wirth *et al*, 2003). During protein synthesis at the ER, the permeability of the translocon for small ions has to be tightly controlled. Accordingly, the ribosome–Sec61 complex is assumed to be impermeable to ions during nascent chain transport (Crowley *et al*, 1994). However, this view was recently challenged by 3D reconstructions after cryo-EM for Sec61/ribosome–complexes, which revealed a gap between Sec61 and the ribosome (Menetret *et al*, 2008; Becker *et al*, 2009). In the empty state after the translocation event, that is when the translocon is still ribosome bound but unoccupied by a polypeptide chain, and in the ribosome-depleted state the translocon complex seems to transiently allow the passage of small molecules and calcium ions (Ca^{2+}) (Roy and Wonderlin, 2003; Flourakis *et al*, 2006; Giunti *et al*, 2007; Ong *et al*, 2007). Furthermore, the mammalian Sec61 complex shows characteristics of an ion channel under these conditions (Simon and Blobel, 1991; Wirth *et al*, 2003; Wonderlin, 2009). These results indicate that, at least in mammals, calcium ions could be lost from the ER during or after the termination of protein translocation.

The controlled release of Ca^{2+} from the ER lumen to the cell cytosol is one of the key factors in the regulation of many physiological processes, including muscle contraction, exocytosis, and apoptosis. In the resting state, the Ca^{2+} concentration in the ER lumen is the result of a balance between Ca^{2+} uptake by sarcoplasmic ER calcium ATPases (SERCAs) (Wuytack *et al*, 2002) and Ca^{2+} leakage currents (Camello *et al*, 2002). Recent studies have proposed that the Sec61 complex may contribute to Ca^{2+} leakage (Lomax *et al*, 2002; van Coppenolle *et al*, 2004; Flourakis *et al*, 2006; Giunti *et al*, 2007). However, uncontrolled leakage of Ca^{2+} through the large, aqueous Sec61 pore would seriously interfere with the capacity of the ER membrane to maintain Ca^{2+} concentrations roughly three to four orders of magnitude higher than in cytosol (Yu and Hinkle, 2000; Smith *et al*, 2001; Alvarez, 2002). In addition, leakage would compromise the regulated

release of calcium from the ER lumen in specific spatial and temporal patterns.

Calmodulin (CaM) is a highly conserved protein with two pairs of EF-hand motifs (Babu *et al*, 1985). The binding of Ca^{2+} to these motifs induces a conformational change in CaM that, in turn, regulates the activity of CaM target proteins in a calcium-dependent manner. Ion channels are a major class of CaM-regulated proteins, particularly those committed to calcium homeostasis (Yamada *et al*, 1995; Zühlke *et al*, 1999; DeMaria *et al*, 2001; Yamaguchi *et al*, 2001; Bähler and Rhoads, 2002; Dick *et al*, 2008; Tadross *et al*, 2008; Wang *et al*, 2008). The IQ motif and the 1-8-14 motif are widely distributed, evolutionarily conserved motifs mediating the binding of CaM to interaction partners (Rhoads and Friedberg, 1997; Puntervoll *et al*, 2003).

Here, we show that Ca^{2+}-CaM can bind to an IQ motif that is present in the cytosolic N-terminus of the α subunit of the Sec61 complex. The binding of Ca^{2+}-CaM to the Sec61 complex triggers closure of the Sec61 channel and is sensitive towards CaM antagonists that interfere with substrate binding of CaM. At the cellular level, the same CaM antagonists stimulate Ca^{2+} leakage from the ER via Sec61 complexes. Molecular modelling and docking analysis of Ca^{2+}-CaM and the ribosome/Sec61 complex support the view that Ca^{2+}-CaM and ribosomes simultaneously bind to the Sec61 complex. This finding is consistent with our observation that Ca^{2+}-CaM does not interfere with cotranslational protein transport into the ER. Thus, CaM contributes to cellular calcium homeostasis by limiting Ca^{2+} leakage from the ER at the level of Sec61 complexes.

Results

CaM binds to a conserved motif of the Sec61α subunit in a calcium-dependent and sequence-specific manner

Using computational prediction services (http://calcium.uhnres.utoronto.ca/ctdb/ctdb/sequence.html) and the eukaryotic linear motif server (http://www.elm.eu.org), we identified an IQ motif in the cytosolic N-terminus of mammalian Sec61α (Figure 1A and B). The motif $_{19}$IQKPERKIQFKEKV$_{32}$ from the Sec61α subunit is highly conserved in higher eukaryotes and compares well with the IQ consensus motif ([IVL]QxxxRxxxx[RK]xx[FILVWY]) found in unconventional myosins, neuromodulin, and neurogranin (Yap *et al*, 2000; Puntervoll *et al*, 2003) and also conforms to the 1-8-14 motif (Table I).

To determine whether CaM binds to this Sec61α IQ motif, we synthesized the corresponding peptide, added a terminal cysteine, and labelled it with a fluorescent dye (Atto488). In fluorescence correlation spectroscopy (FCS) experiments (according to Petrasek and Schwille, 2008), the CaM–IQ_{488} complex formation was detected by an increase in the diffusion time (τ_D) for the IQ_{488} peptide. After the addition of 1 μM CaM in the presence of 10 μM $CaCl_2$, τ_D increased from 148 ± 5 μs to 199 ± 4 μs (Figure 1C). To amplify the signal, we increased the molecular mass of CaM by glutathione-S-transferase (GST) fusion. With the addition of 4 μM GST-CaM, τ_D further increased to 297 ± 8 μs (Figure 1C). We found that CaM binding to the IQ_{488} peptide in the presence of saturating calcium concentrations (4 mM) occurred via a single-site binding mechanism (Hill slope: 1.1 ± 0.19; K_D 121 ± 28 nM; Figure 1D) and GST-CaM bound to the IQ_{488} peptide with a Hill slope of 0.88 ± 0.07 and a K_D of 115 ± 12 nM (Figure 1E). In the absence of Ca^{2+}, CaM did not interact with the IQ_{488} peptide at comparable concentrations (Figure 1D and E). We concluded that CaM bound to the Sec61α IQ peptide in a calcium-dependent manner and with high affinity.

Next, we tested the sequence specificity of calcium-dependent CaM interactions with the Sec61α IQ motif. We synthesized IQ peptides with alanines in place of conserved amino acids and these were spotted on a cellulose membrane (Hilpert *et al*, 2007). Binding assays were carried out in the presence and absence of Ca^{2+} (Figure 1F). Consistent with the FCS results, the wild-type Sec61α IQ motif bound ^{14}C-labelled GST-CaM in the presence of free calcium (Figure 1F, spots 1, 7, and 10; defined as 100% binding). When Ca^{2+} was chelated with EGTA, GST-CaM binding was nearly abolished (spots 1, 7, and 10; 17 ± 5% binding). The exchange of the conserved residues to alanine at positions 7 and 11 drastically reduced CaM binding (spots 5 and 6; 24 ± 4.8% binding). However, modifying the residues at positions 2 and 3 did not alter CaM binding (spots 2, 3, and 4; 80 ± 16% binding). As negative controls, the N-terminus of the Sec61α ortholog in *Escherichia coli*, SecY, and the N-terminus of the human TRAM protein were analysed. As expected, the peptides from the SecY and TRAM proteins did not bind CaM (spots 8 and 9; 12 ± 7% and 2 ± 0.2% binding, respectively). When ^{14}C-labelled GST was added to the IQ constructs as a control, no binding was observed (Figure 1F). We concluded that CaM bound to the Sec61α IQ peptide in a sequence-specific and calcium-dependent manner.

CaM interacts with the native Sec61 complex

We studied the binding of CaM to native Sec61 complexes, present in rough microsomes (RM), by flotation in sucrose gradients. GST-CaM was incubated with RM, or RM that had been pretreated with puromycin and high salt in order to remove ribosomes (termed PKRM; Görlich and Rapoport, 1993), or purified and reconstituted Sec61 complex (Görlich and Rapoport, 1993), in the presence or absence of Ca^{2+}. Subsequently, the samples were adjusted for a high sucrose concentration, placed on the bottom of centrifuge tubes and covered with the sucrose gradient. After centrifugation, fractions were taken and analysed by SDS–PAGE, western blot, and immunodetection of GST-CaM and Sec61β. GST-CaM floated with RM in the presence, and perhaps to a lesser extent in the absence of Ca^{2+} (Figure 2B and C; 3.47 ± 0.84% and 1.47 ± 0.59%, respectively, flotation). In addition, we observed that a CaM antagonist that interferes with substrate binding, such as trifluoperazine (Johnson and Fugman, 1983; Vandonselaar *et al*, 1994), interferes with binding of GST-CaM to RM in the presence of Ca^{2+} (Figure 2D; 0.51 ± 0.11%). GST-CaM also floated with PKRM and reconstituted Sec61 complex in the presence of Ca^{2+} (Figure 2E and G; 3.57 ± 0.68% and 29.37 ± 4.56%, respectively, flotation), but not without any membranes or with protein-free liposomes (Figure 2A and F; 0.22% and 0.75 ± 0.47%, respectively, flotation). We concluded that the CaM-binding site in the membrane resident Sec61 complex was active and accessible to CaM even in the presence of ribosomes and that the interaction of CaM with the Sec61 complex involved CaM's substrate-binding site.

Alternatively, interaction of CaM with native Sec61 complex was analysed by employing the reagent FeBABE that can

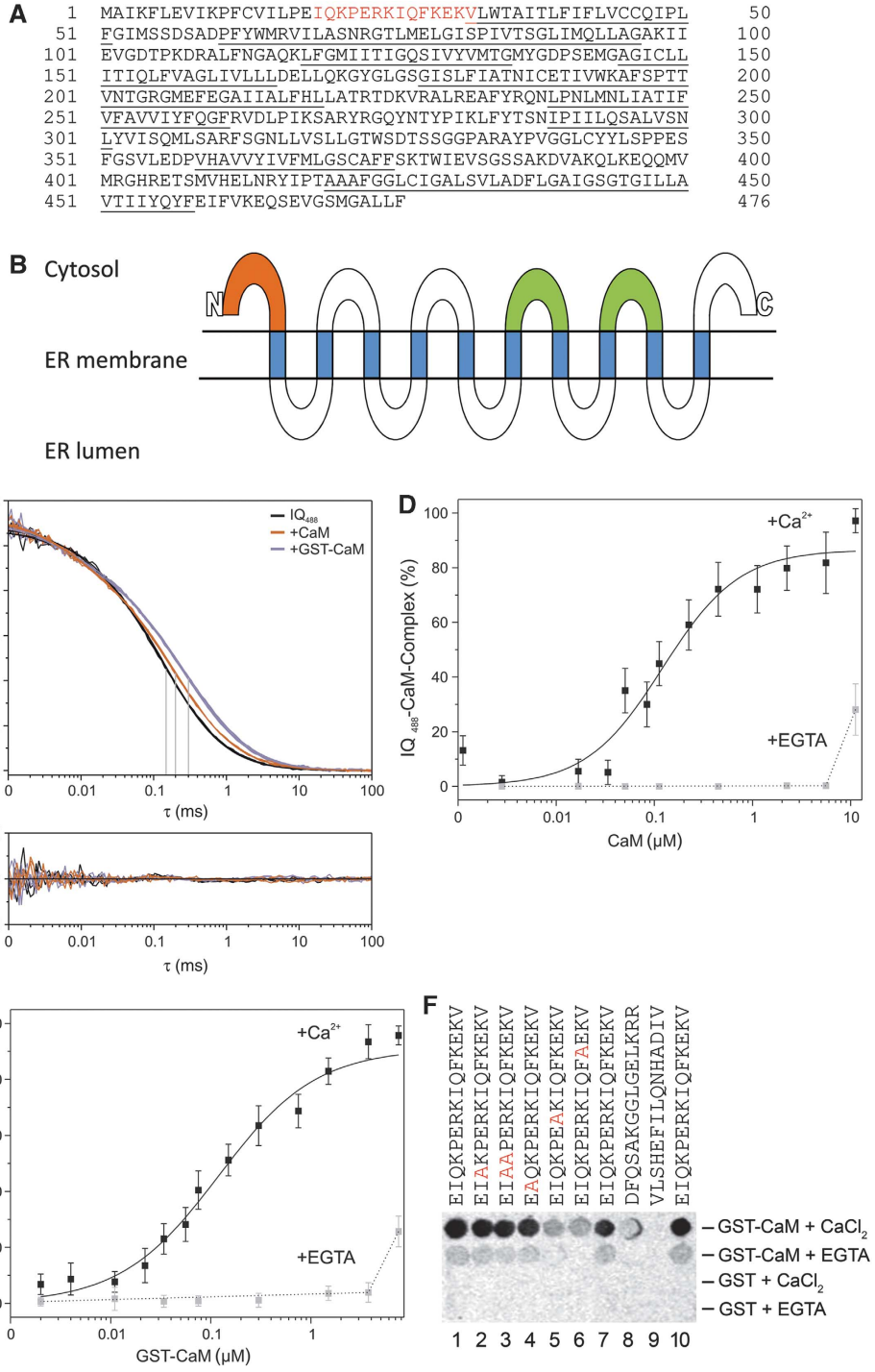

Figure 1 Sec61α IQ motif and its interactions with calmodulin. (**A**) The IQ motif (red), as proposed for unconventional myosins and others (Rhoads and Friedberg, 1997), that was identified in the sequence of the Sec61α subunit from *Canis lupus familiaris*. Predicted transmembrane helices are underlined. (**B**) Predicted membrane topology of the mammalian Sec61α subunit. The IQ motif is indicated in red, the two cytosolic loops that most intimately contact with the ribosomal exit tunnel according to cryo-EM (Menetret *et al*, 2008; Becker *et al*, 2009) are indicated in green. Predicted transmembrane helices are shown in blue. N, N-terminus; C, C-terminus. (**C**) Fitted autocorrelation functions and residuals for the IQ_{488} peptide in the presence of 10 μM $CaCl_2$ with the addition of 1 μM CaM or 4 μM GST-CaM. (**D**, **E**) Formation of the IQ_{488}–CaM complex with increasing concentrations of CaM (**D**) or GST-CaM (**E**) in the presence of 4 mM $CaCl_2$ or 10 mM EGTA. Error bars represent s.d. (**F**) IQ-peptide spots bound by ^{14}C-labelled GST-CaM and ^{14}C-labelled GST in the presence of 1 mM $CaCl_2$ or 4 mM EGTA. Spots 1–7 and 10 correspond to the Sec61α IQ peptide (*Homo sapiens*). Amino acids were exchanged as indicated. Spots 8 and 9 correspond to the respective region of SecY (*E. coli*) and TRAM (*H. sapiens*) proteins, respectively. We note that the analysis of the various peptides was carried out three times. Furthermore, we note that similar results were obtained when unlabelled GST-CaM and anti-GST antibodies in combination with POD-coupled anti-rabbit antibodies, ECL™, and luminescence imaging were employed (data not shown).

Table I Sequence alignments for Sec61α and SecY

Species	ID	IQ motif
Homo sapiens	P61619	$_{-19}$IQKPERKIQFKEKV$_{32-}$
Canis lupus familiaris	NP_001000315.1	$_{-19}$IQKPERKIQFKEKV$_{32-}$
Mus musculus	P61620	$_{-19}$IQKPERKIQFKEKV$_{32-}$
Gallus gallus	XP_414364.2	$_{-120}$IQKPERKIQFKEKV$_{133-}$
Danio rerio	NP_963871.1	$_{-19}$IQKPERKIQFKEKV$_{32-}$
Oncorhynchus mykiss	Q98SN9	$_{-19}$IQKPERKIQFKEKV$_{32-}$
Xenopus laevis	Q7ZX87	$_{-19}$IQKPERKIQFKEKV$_{32-}$
Drosophila melanogaster	Q8STG9	$_{-19}$IAKPERKIQFREKV$_{32-}$
Arabidopsis thaliana	NP_174225.2	$_{-21}$VQSADRKIPFREKV$_{34-}$
Oryza sativa	NP_001049359.1	$_{-21}$VQSADRKIPFREKV$_{34-}$
Plasmodium falciparum	XP_001350175.1	$_{-18}$VQSPDRKLPFKEKL$_{31-}$
Saccharomyces cerevisiae	P32915	$_{-20}$VIAPERKVPYNQKL$_{33-}$
Escherichia coli	P0AGA3	$_{-10}$QSAKGGLGELKRRL$_{23-}$
Thermus thermophilus	Q72I24	$_{-5}$FWSALQIPELRQRV$_{18-}$
Thermotoga maritima	Q9X1I9	$_{-5}$FKNAFKIPELRDRI$_{18-}$
Salmonella choleraesuis	Q57J52	$_{-10}$QSAKGGLGELKRRL$_{23-}$
Bacillus subtilis	P16336	$_{-5}$ISNFMRVSDIRNKI$_{18-}$
Methanococcus jannaschii	Q60175	$_{-14}$VELPVKEITFKEKL$_{27-}$
Methanobacterium thermoautotrophicum	O26134	$_{-18}$VKSPGYRVPFREKL$_{31-}$
Methanosarcina acetivorans	Q8TRS4	$_{-17}$VASPEKHVHFKDKL$_{30-}$
Halobacterium salinarium	Q9HPB1	$_{-17}$VERPEGHVPFRRKM$_{30-}$

Representative sequences were selected for ClustalW2 multiple sequence alignments. The IQ motif and homolog sequences are shown for eukaryotes, eubacteria, and archaea.

be attached to a bait protein and used to artificially hydrolyze nearby peptide bonds in a prey protein (Ghaim *et al*, 1995). GST-CaM was derivatized with FeBABE, incubated with reconstituted Sec61 complex, and activated with ascorbate and peroxide (i.e. converted to active protease). Subsequently, the samples were analysed by SDS–PAGE, western blot, and immunodetection of Sec61α with an antibody that is directed against the C-terminus of Sec61α. Derivatized and activated GST-CaM cleaved Sec61α in the presence and absence of Ca^{2+} to the indicated C-terminal 20 kDa fragment plus two less abundant fragments of larger molecular mass (Figure 2H, lanes 3 and 5). Without FeBABE attachment, there was no proteolytic cleavage observed (Figure 2H, lane 2). Furthermore, there was no proteolytic cleavage observed when FeBABE modified and activated GST was employed (Figure 2H, lane 4). Thus, the artificial protease approach confirmed the conclusion that the CaM-binding site in the native Sec61 complex is accessible to CaM. However, we note that evidence for a direct interaction between CaM and Sec61 in its native context remains to be fully explored.

CaM binding induces calcium-dependent Sec61-channel closure

We also characterized the effect of CaM on Sec61-channel activity using electrophysiology. Vesicles containing native or reconstituted Sec61 complexes were osmotically fused to lipid bilayers as previously described (Wirth *et al*, 2003). In transport-competent vesicles that were derived from RM, single-channel activities were observed after treatment with puromycin, which caused the termination of translocation and the dissociation of ribosomes (Figure 3A, middle trace; Supplementary Figures S1 and S2). The addition of 500 nM CaM to RM channels led to closure of the pore in the presence of calcium (Figure 3A, lower trace). In agreement with the FCS results, we found that a Ca^{2+} concentration of 10 μM was sufficient to induce CaM-mediated channel closure (Figure 3B). In the absence of calcium, no channel closure was observed with the addition of CaM (Figure 3C). A statistic evaluation of the CaM effect on the channel open probability is shown in Figure 3D. Comparing the open probability before and after the addition of CaM showed an explicit closure of the channel for all membrane potentials examined. Again, the closure of the Sec61 complex by CaM was strictly dependent on free Ca^{2+}; in the presence of 10 mM EGTA, we observed no reduction in the open probability with the addition of 500 nM CaM (Figure 3D). An additional experiment demonstrated that the observed effects involved a CaM/Sec61 interaction. With proteoliposomes that contained only purified Sec61 complexes, the observed effect was indistinguishable from the results with RM preparations (Figure 3E).

Therefore, both the binding of free Ca^{2+} to CaM and the binding of CaM to Sec61 are essential for the regulation of the open probability. In contrast, the presence of calcium-free apocalmodulin had no effect on the Sec61 channel, consistent with the IQ motif-binding studies.

CaM antagonists enhance calcium leakage from the ER in intact cells

Under resting conditions of the cell, the cytosolic-free Ca^{2+} concentration is low due to the action of plasma membrane pumps and exchangers (50–100 nM). Simultaneously, the free Ca^{2+} concentration in the ER lumen is high, basically because of the action of SERCA (100–800 μM). This Ca^{2+} distribution is constantly challenged by the so-called calcium leak, a passive calcium efflux from the ER. The drug thapsigargin irreversibly inhibits SERCA, thereby unmasking the leak pathway. The leakage of Ca^{2+} from the ER can be visualized as an increase in the cytosolic calcium concentration by utilizing a Ca^{2+} indicator, such as FURA-2, in intact cells in the absence of extracellular calcium. Indirect evidence from various laboratories suggests that the Sec61 complex contributes to the leak after termination of protein translocation (Lomax *et al*, 2002; van Coppenolle *et al*, 2004;

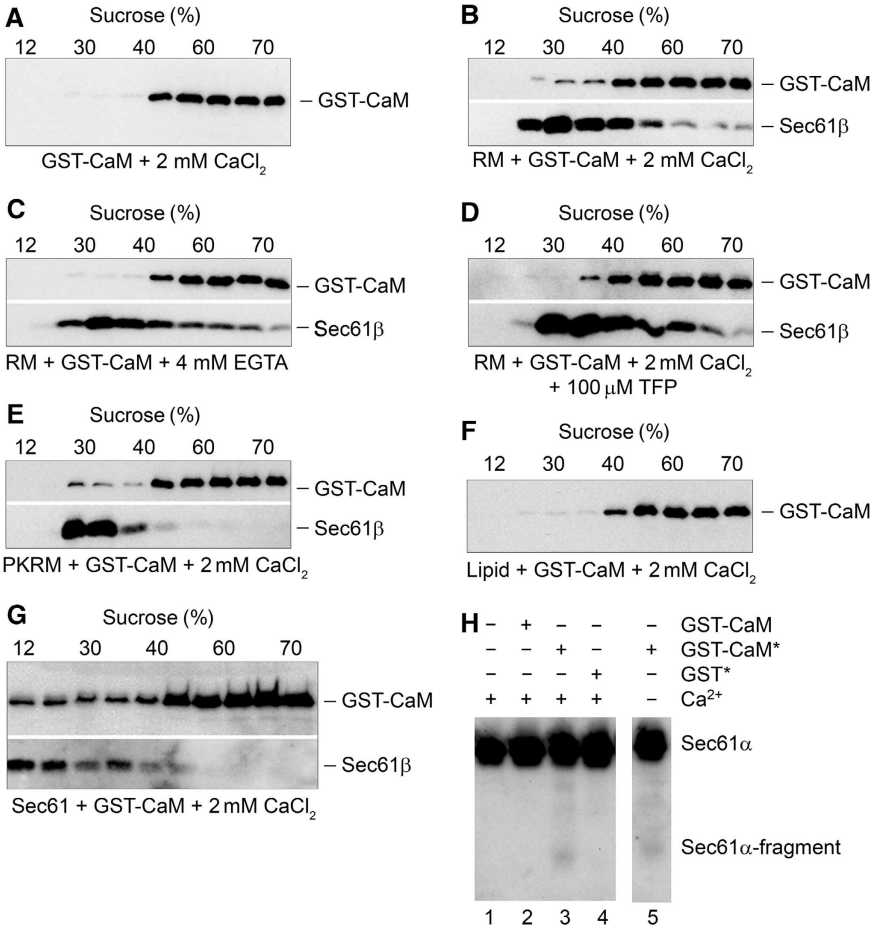

Figure 2 Sec61 complex interactions with calmodulin. (**A**) Flotation analysis of GST-CaM in the presence of calcium in sucrose gradients. (**B**, **C**) Coflotation experiments in sucrose gradients of canine pancreatic rough microsomes (RM) with GST-CaM in the presence (**B**) or absence (**C**) of calcium. (**D**) Coflotation experiments in sucrose gradients of RM with GST-CaM in the simultaneous presence of calcium and trifluoperazine (TFP). (**E**, **G**) Coflotation experiments in sucrose gradients of PKRM (**E**) and Sec61 proteoliposmes (**G**) with GST-CaM in the presence of calcium. (**F**) Coflotation experiments of protein-free liposomes with GST-CaM in the presence of calcium. We note that the analysis was carried out between three (buffer, liposomes) and five times (RM, PKRM, Sec61 proteoliposomes) with similar results. (**H**) GST-CaM and GST were derivatized with FeBABE according to the manufacturer's protocol (indicated with asterisk) or were left underivatized, and incubated with Sec61 proteoliposomes for 30 min at room temperature in the presence or absence of calcium as indicated. Activation with ascorbate and peroxide was carried out for 30 s. We note that the analysis was carried out three times with similar results. All samples were analysed by SDS–PAGE, western blotting, and immunodetection of GST-CaM, Sec61α, or Sec61β in combination with POD-coupled anti-rabbit antibodies, ECL™, and luminescence imaging as indicated. In all panels, the areas of interest for single western blots and gels are shown, in panels **B** through **E** and **G** the two parts that are divided by a white space represent two consecutive immunodetections for the same blots.

Flourakis *et al*, 2006; Giunti *et al*, 2007). Based on the above *in vitro* experiments, we expected CaM to contribute to limiting the Sec61-mediated calcium efflux under these conditions and for CaM antagonists to enhance the leak. Therefore, we investigated whether the presence of CaM antagonists that interfere with substrate binding by CaM, ophiobolin A (Leung *et al*, 1984; Au *et al*, 2000) and trifluoperazine (Johnson and Fugman, 1983; Vandonselaar *et al*, 1994), enhance Ca^{2+} efflux from the ER in the presence of thapsigargin. In Ca^{2+} imaging experiments with FURA-2, HeLa cells were treated with one of the two CaM antagonists for 10 min and, subsequently, Ca^{2+} was released by applying thapsigargin in the absence of external Ca^{2+}. The two CaM antagonists ophiobolin A and trifluoperazine had similar enhancing and significant effects on the thapsigargin-induced calcium efflux (Figure 4A, B, and H). Thus, CaM contributes to reducing Ca^{2+} leakage from the ER under normal conditions.

Next, we asked if this effect of CaM can be linked to the Sec61 complex. Therefore, HeLa cells were treated with two different siRNAs directed against the coding (*SEC61A1*) or untranslated region (*SEC61A1*-UTR) of *SEC61A1* or a negative control siRNA for 96 h. We note that at this time point the total number of *SEC61A1* silenced cells was somewhat lower as compared to control cells (Supplementary Figure S3A). However, the *SEC61A1* silenced cells did not show dramatic signs of siRNA toxicity, that is according to the Nuclear-ID assay there was no drop in cell viability as compared to cells that had been treated with control siRNA (Supplementary Figure S3B). The results of calcium imaging experiments for cells with the control siRNA were indistinguishable from those of the untreated cells (Figure 4C, D, and H). For both ophiobolin A and trifluoperazine, silencing of *SEC61A1* by either one of the two siRNAs had a similar inhibitory effect on the thapsigargin-induced Ca^{2+} efflux (Figure 4E, F, and H). Based on western blot analysis, the silencing efficiency of

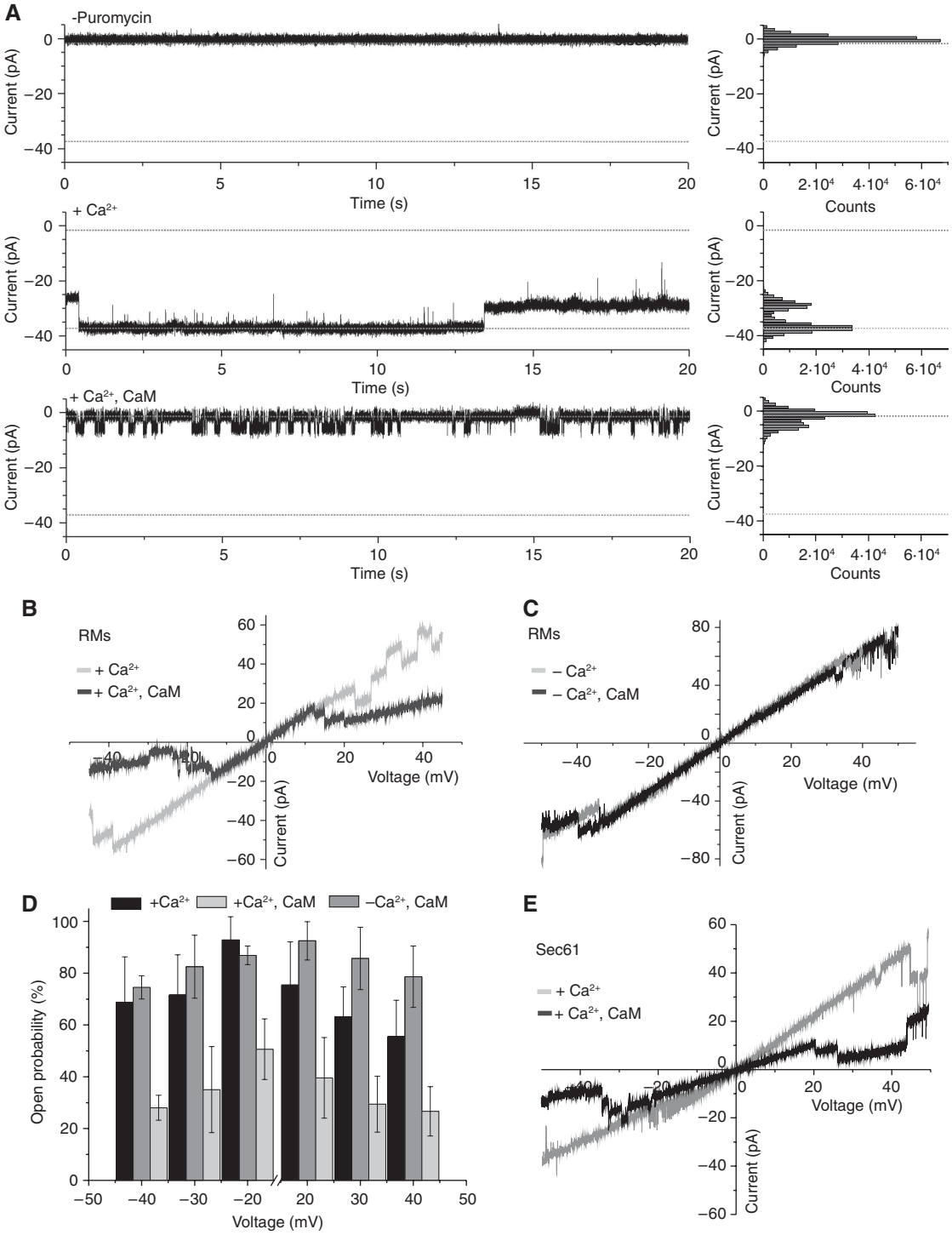

Figure 3 Electrophysiological properties of Sec61 in the presence of calmodulin. (**A**) Current traces from rough microsomes (RM) preparations before (middle trace) and after (lower trace) the addition of 500 nM calmodulin to both compartments (*cis/trans*), at a membrane potential of −30 mV and in the presence of 13 mM $CaCl_2$ and 200 μM puromycin. The upper trace shows a control experiment in the absence of puromycin. The frequency histograms (right panels) depict the main current levels observed in the recordings shown in the left panels. Baseline and the high conductance state of the Sec61 channel are indicated with dashed lines. (**B**) Voltage ramp recording of a RM channel before (grey) and after (black) the addition of 500 nM calmodulin *cis/trans* in the presence of 10 μM $CaCl_2$. Measurements were performed in 100 mM KCl, 10 mM Mops/Tris (pH 7.0) *cis/trans* and 200 μM puromycin. (**C**) Voltage ramp recording of a bilayer containing a single-Sec61 channel from RM vesicles before (grey) and after (black) the addition of 500 nM calmodulin *cis/trans* in the absence of Ca^{2+} (10 mM EGTA). Measurements were performed in 100 mM KCl, 10 mM Mops/Tris (pH 7.0) *cis/trans* and 200 μM puromycin. (**D**) Open probability of the Sec61 channel from RM vesicles before and after the addition of 500 nM calmodulin *cis/trans* in the presence (13 mM $CaCl_2$) or absence (10 mM EGTA) of Ca^{2+} ($n = 6$–9 bilayers). Error bars represent s.d. Measurement conditions: 100 mM KCl, 10 mM Mops/Tris (pH 7.0), 200 μM puromycin. (**E**) Voltage ramp recording of the purified Sec61 complex before (grey) and after (black) the addition of 1 μM calmodulin *cis/trans* in the presence of 13 mM $CaCl_2$. The experiment was performed under symmetrical buffer conditions of 100 mM KCl, 10 mM EGTA, 10 mM Mops/Tris (pH 7.0), and 200 μM puromycin.

both siRNAs was above 85% (Figure 4G). Thus, CaM contributes to reducing Ca^{2+} leakage from the ER at the level of the Sec61 complex.

In order to confirm this conclusion, we attempted expression of the *SEC61A1* cDNA, lacking the UTR of the *SEC61* gene, in the presence of the *SEC61A1*–UTR siRNA and observed that it indeed rescues the phenotype of *SEC61A1* silencing, that is partially restores the effects of ophiobolin A and trifluoperazine (Figure 5B). Based on western blot analysis, the complementation efficiency of the *SEC61A1* expression plasmid was around 85% (Figure 5A). In order to link the CaM effect to the IQ motif in Sec61α, we asked how a *SEC61A1* cDNA with a mutated IQ motif behaves in the rescue experiment. For this, the two mutations that were observed to be effective in the peptide-binding experiments (Figure 1F) were simultaneously introduced into the *SEC61A1* cDNA. Based on western blot analysis, the complementation efficiency of the *SEC61A1* expression plasmid was around 50% (Figure 5C). In contrast to Sec61α, mutant Sec61α R24A/K29A did not restore the effects of the CaM antagonists in the presence of the *SEC61A1*–UTR siRNA (Figure 5D). Furthermore, mutant Sec61α R24A/K29A led to an increased Ca^{2+} efflux from the ER in the presence of thapsigargin *per se*, that is irrespectively of the used siRNA and in the absence of any CaM antagonist (buffer controls show 60% increase in Figure 5D versus Figure 6B). We suggest that this is due to the presence of Sec61 complexes that cannot be controlled by CaM because of a mutated IQ motif.

Ca^{2+}-CaM does not interfere with the transport of presecretory proteins into microsomes

The question arose of whether Ca^{2+}-CaM affects the Sec61-mediated translocation of polypeptides into microsomes. As the calcium affinity of CaM is in the range of 10–100 μM, we first investigated whether Ca^{2+} affects protein transport in reticulocyte lysate. As reticulocyte lysate is routinely pretreated with a calcium-dependent ribonuclease that is inactivated by an excess of EGTA, transport had to be carried out under posttranslational conditions in the presence of excess Ca^{2+}. Nascent preprolactin (ppl-86mer) was synthesized in the presence of [^{35}S]methionine, and then the translation reaction was supplemented with microsomes and divided into several aliquots. Where indicated the aliquots were simultaneously supplemented with Ca^{2+}. In order to allow membrane targeting of the ribosome–SRP–nascent chain complexes, the aliquots were incubated further. The microsomes were re-isolated by centrifugation, re-suspended in buffer, and incubated for an additional 20 min at 30°C in the absence or presence of puromycin. Subsequently, the samples were subjected to protease treatment or chemical cross-linking. All samples were subjected to SDS–PAGE and phosphorimaging (Figure 6A through D). As expected, in the presence of microsomes and absence of Ca^{2+}, ppl-86mer productively associated with the Sec61 complex (i.e. was protected by the ribosome against externally added protease and could be cross-linked to Sec61α in the absence of puromycin (Figure 6A, lane 2; Figure 6B, lane 1)). Subsequently, ppl-86mer was chased to the mature ER lumen form pl-56mer by the addition of puromycin (i.e. was protected by the microsomal membrane against externally added protease and could not any longer be cross-linked to Sec61α (Figure 6A, lane 4; Figure 6B, lane 2)). However, at effective Ca^{2+} concentrations of 200 and 800 μM, ppl-86mer associated with the Sec61 complex less efficiently (Figure 6A, lanes 6 and 10; Figure 6B, lanes 3 and 5) and, therefore, could not efficiently be chased to pl-56mer by the subsequent addition of puromycin (Figure 6A, lanes 8 and 12; Figure 6B, lanes 4 and 6). In addition, preprocecropin mutant (ppcec) was analysed as a truely posttranslationally transported model precursor polypeptide. The precursor was completely synthesized and incubated with microsomes and Ca^{2+} as indicated (Figure 6E). Subsequently, the samples were subjected to protease treatment, SDS–PAGE and phosphorimaging. In the absence of Ca^{2+}, ppcec was inserted into the microsomal membrane and processed to mature pcec (Figure 6E, lane 3). Furthermore, pcec was protected against externally added protease, suggesting that it was imported into microsomes (Figure 6E, lane 4). In the presence of Ca^{2+}, ppcec was not processed and imported (Figure 6E, lanes 9 and 10). Thus, submillimolar concentrations of Ca^{2+} inactivated the Sec61 complex with respect to its cotranslational and posttranslational protein transport ability, as we previously observed for lanthanum ions (Erdmann *et al*, 2009).

Next, we investigated whether Ca^{2+}-CaM affects protein transport into microsomes, that is was responsible for the observed inhibitory effect of Ca^{2+}. First, the transport of ppl-86mer was carried out in the simultaneous presence of both Ca^{2+} (200 μM) and CaM (60 μM). After the addition of CaM to the transport reaction, the inhibitory effect of Ca^{2+} on cotranslational transport was partially relieved (Figure 6C and D). Second, transport of ppcec was carried out under similar conditions. After the addition of CaM to the transport reaction, the inhibitory effect of Ca^{2+} on posttranslational transport was partially relieved (Figure 6E, lanes 7 and 8). Thus, CaM-bound Ca^{2+}, and the Ca^{2+}-CaM did not interfere with protein transport into microsomes.

Discussion

During protein synthesis at the ER, the permeability of the translocon for small ions has to be tightly controlled. Therefore, the ribosome–Sec61 complex is assumed to be impermeable to ions during nascent chain transport (Crowley *et al*, 1994). By contrast, in the empty state after the translocation event, that is when the translocon is still ribosome bound but unoccupied by a polypeptide chain, as well as in the ribosome-depleted state, the translocon complex seems to allow the passage of small molecules and Ca^{2+} (Lomax *et al*, 2002; Roy and Wonderlin, 2003; Flourakis *et al*, 2006; Giunti *et al*, 2007; Ong *et al*, 2007). In addition, the mammalian Sec61 complex comprises an ion channel under these conditions (Simon and Blobel, 1991; Wirth *et al*, 2003; Wonderlin, 2009), while the bacterial homolog SecYEG does not exhibit channel activity in electrophysiological experiments (Saparov *et al*, 2007). These results show that, depending upon the rate of protein synthesis, calcium ions could be lost from the ER during or after termination of protein translocation.

Electrophysiological studies have shown that local cytosolic Ca^{2+} concentrations in the range of 1–10 μM are sufficient to activate IP_3- and Ryanodine receptors in the ER membrane, thereby triggering calcium-induced calcium release (CICR) (Xu *et al*, 1996; Boehning *et al*, 2001; Foskett *et al*, 2007). An enhanced local calcium concentration at the cytosolic face of the ER membrane due to uncontrolled leak efflux

through the Sec61 channel could dramatically affect CICR and cellular calcium signalling. This is even more obvious considering that calcium ions conducted by an ion channel generate calcium nanodomains in the cytosolic vicinity of the pore mouth with Ca^{2+} concentrations that can exceed the concentration of the surrounding bulk solution by three orders of magnitude with concentrations of up to 20–50 μM (Rizzuto and Pozzan, 2006). The formation of these nanodomains originates from much faster permeation through the aqueous pore of an ion channel compared to the high

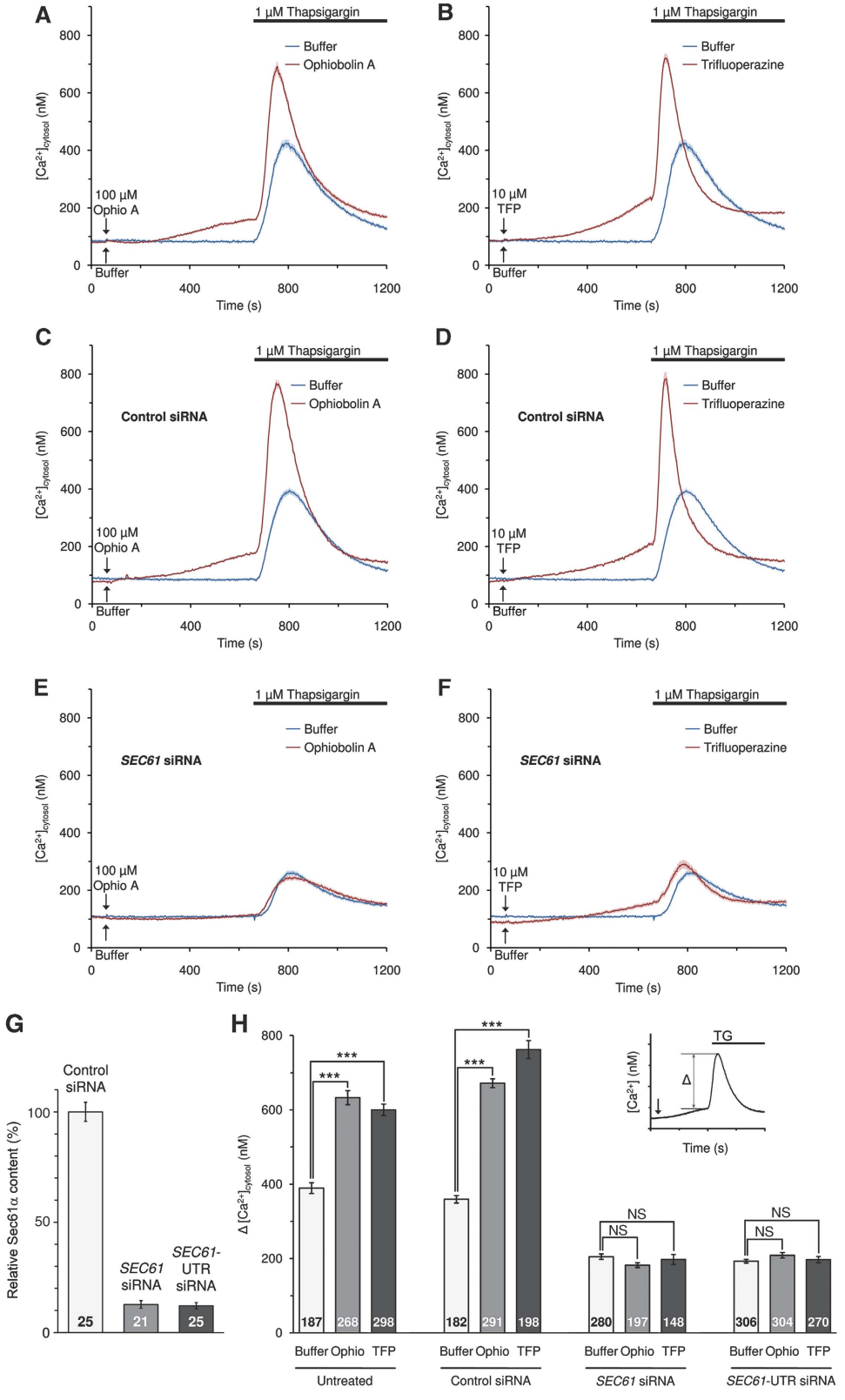

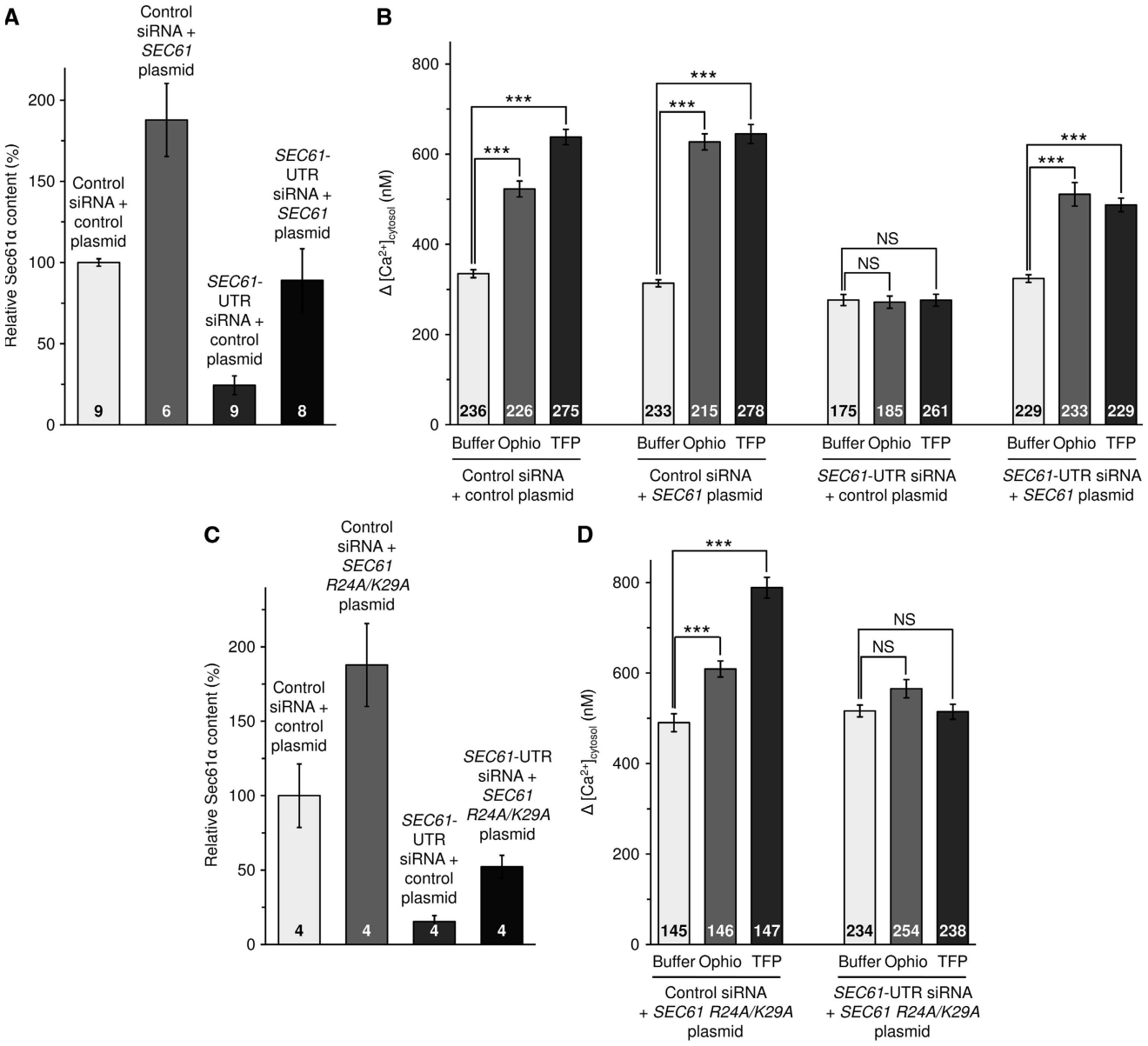

Figure 5 Live cell calcium imaging of HeLa cells in the presence of *SEC61A1* plasmids and CaM antagonists. (**A**–**D**) Cells were treated with control siRNA or *SEC61A1*-UTR siRNA as described in the legend to Figure 4 for 48 h and then transfected with either control vector, or *SEC61A1* expression plasmid (**A**, **B**), or mutant *SEC61A1* expression plasmid (**C**, **D**). After 48 h, calcium imaging experiments were carried out as in Figure 4. Silencing and overexpression were evaluated by western blot analysis as in Figure 4 (**A**, **C**). Statistical analysis of the changes in the cytosolic Ca^{2+} concentration after the addition of thapsigargin was carried out as described in the legend to Figure 4 (**B**, **D**). Average values are given, error bars represent standard errors of the means (s.e.m.). *P* values <0.001 were defined as significant by unpaired *t* test and are indicated by three asterisks (***), NS, not significant. The numbers of cells that were analysed are indicated.

Figure 4 Live cell calcium imaging of HeLa cells in the presence of *SEC61A1* siRNA and CaM antagonists. HeLa cells were loaded with the calcium indicator FURA-2 AM and experiments were carried out with a Ca^{2+}-free buffer containing 0.5 mM EGTA. (**A**, **B**) Naive HeLa cells were treated with the indicated CaM antagonist or with the Ca^{2+}-free buffer. Ca^{2+} release was initiated by applying thapsigargin in the absence of external Ca^{2+}. Error bars represent standard errors of the means (s.e.m.). (**C**–**F**) HeLa cells were treated with one of the two siRNAs directed against *SEC61A1* (**E**, **F**) or a negative control siRNA (**C**, **D**) for 96 h as indicated and calcium-imaging experiments were carried out as above. (**G**) Silencing was evaluated by western blot analysis using antibodies that were directed against Sec61α and β-actin (loading control). The primary antibodies were visualized by using ECL™ Plex secondary antibodies and fluorescence imaging. Average values are given, error bars represent standard errors of the means (s.e.m.). The numbers of experiments that were analysed are indicated. (**H**) Statistical analysis of the changes in the cytosolic Ca^{2+} concentration after the addition of thapsigargin (as indicated by the insert) in the experiments presented in **A** through **F**, plus the experiments with the second *SEC61A1* siRNA. *P*-values <0.001 were defined as significant by unpaired *t*-test and are indicated by three asterisks (***), NS, not significant. The numbers of cells that were analysed are indicated. The experiments were carried out for four different batches of HeLa cells over a period of 4 months, and two coverslips with at least 20 cells were analysed for each condition in a single experiment. Average values are given, error bars represent standard errors of the means (s.e.m.).

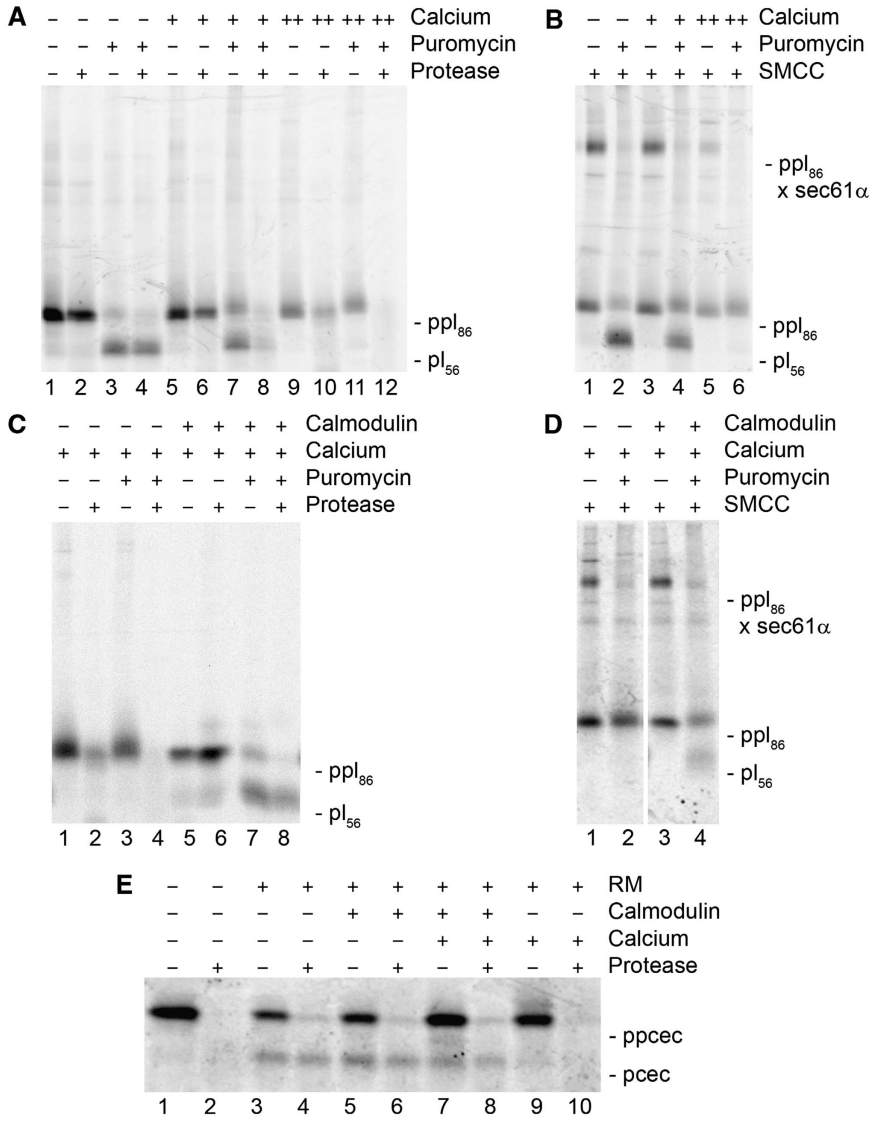

Figure 6 Effect of calcium and calmodulin on cotranslational and posttranslational protein transport into canine pancreatic microsomes. (**A**–**D**) Nascent preprolactin (ppl-86mer) was synthesized in reticulocyte lysate in the presence of [^{35}S]methionine. The translation reaction was supplemented with microsomes and divided into several aliquots. (**A**, **B**) The aliquots were simultaneously supplemented with Ca^{2+} at final concentrations of 200 μM (**A**, lanes 5–8, **B**, lanes 3 and 4) or 800 μM (**A**, lanes 9–12, **B**, lanes 5 and 6) as indicated. (**C**, **D**) The aliquots were simultaneously supplemented with Ca^{2+} at a final concentration of 200 μM (**C**, lanes 1–8, **D**, lanes 1–4) and 60 μM CaM (**C**, lanes 5–8, **D**, lanes 3 and 4) as indicated. For comparison, the physiological concentrations of CaM vary between 3 and 30 μM. The aliquots were incubated an additional 20 min at 30°C. Then the microsomes were re-isolated by centrifugation, re-suspended in cross-linking buffer, and incubated another 20 min at 30°C in the absence or presence of puromycin. Subsequently, the samples were subjected to treatment with proteinase K (**A**, **C**) or to chemical cross-linking (**B**, **D**). (**E**) Mutant preprocecropin (ppcec) was synthesized in reticulocyte lysate in the presence of [^{35}S]methionine. Where indicated, the translation reaction was supplemented with microsomes (RM) and divided into several aliquots. The aliquots were simultaneously supplemented with 200 μM Ca^{2+} and 60 μM CaM as indicated. After incubation for 30 min at 30°C, the samples were subjected to treatment with buffer or protease. All samples were subjected to SDS–PAGE and phosphorimaging. (**E**) Only the area of interest for a single gel is shown.

Ca^{2+}-buffer capacity of the cytosol resulting in slow lateral diffusion of Ca^{2+} ions (Allbritton *et al*, 1992).

Recent publications have provided evidence that the Sec61 channel mediates passive calcium efflux from the intact ER (Lomax *et al*, 2002; Van Coppenolle *et al*, 2004; Flourakis *et al*, 2006; Ong *et al*, 2007), even in the presence of the luminal chaperone and proposed Sec61 gatekeeper BiP (Hamman *et al*, 1998; Alder *et al*, 2005). Whether the observed calcium leakage occurs despite BiP regulation, or is mediated by channels not interacting with BiP, has to be determined. In the light of recent 3D reconstructions of Sec61/ribosome complexes after cryo-EM, which demonstrated a gap between Sec61 and the ribosome (Menetret *et al*, 2008; Becker *et al*, 2009), the physiological necessity for an additional mechanism to prevent Ca^{2+} loss from the ER is evident.

Our data show that CaM interacts with the Sec61 translocon in a sequence-specific manner. We demonstrated that CaM binds to an IQ motif in the cytosolic N-terminus of the Sec61α subunit with high affinity and in a calcium-dependent manner, but not to the bacterial ortholog SecY. This finding was expected because: (i) eubacteria or archaea do not

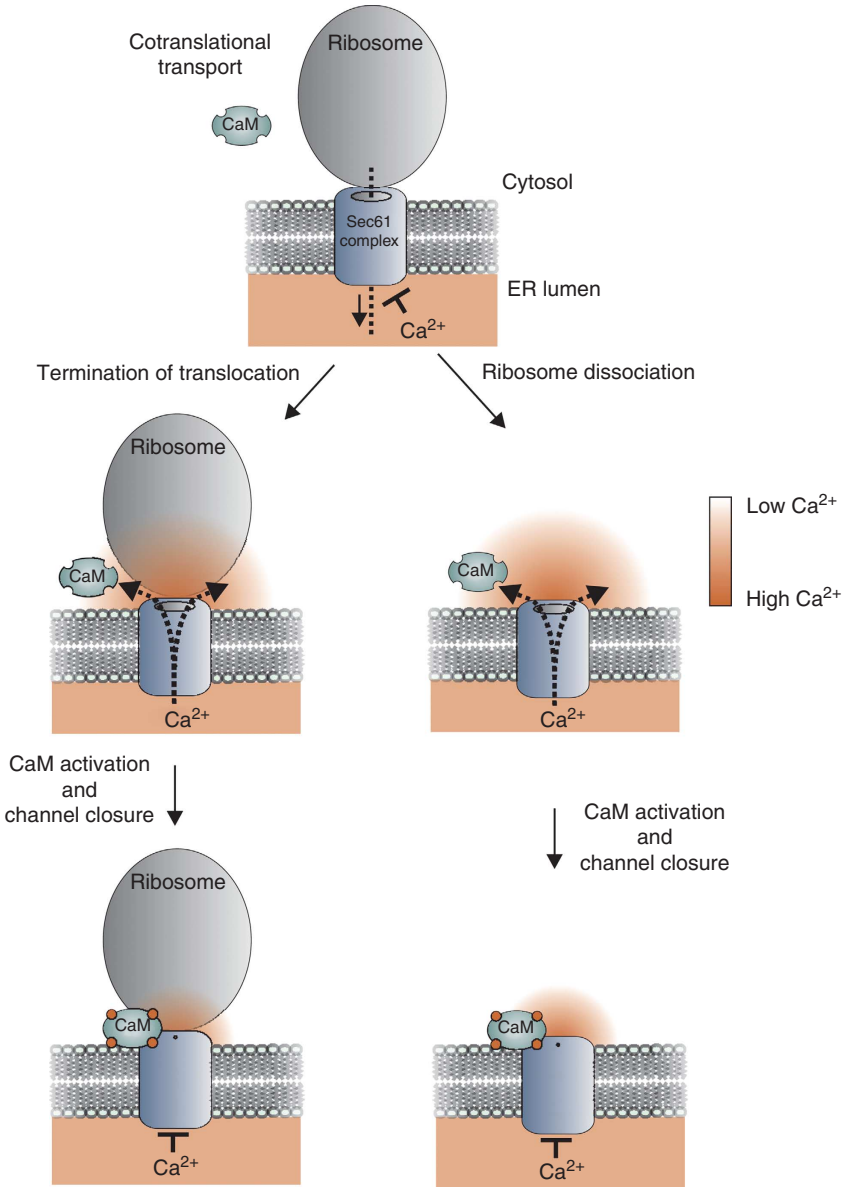

Figure 7 Model for a calmodulin-mediated, calcium-dependent inactivation (CDI) mechanism of Sec61 Ca^{2+} conductance. The Sec61 complex is assumed to be impermeable to ions during cotranslational protein transport, sealed by an ion-tight connection with the ribosome and/or by the ER-lumenal chaperone BiP (Crowley *et al*, 1994; Hamman *et al*, 1998). After translocation, inactive ribosomes remain stably associated with the translocase (Potter and Nicchitta, 2002; Schaletzky and Rapoport, 2006) or dissociate from the complex. Under these conditions, Ca^{2+} ions permeate the channel and accumulate at a calcium nanodomain in the cytosolic vicinity of the pore mouth. Ca^{2+} ions bind to, and thereby activate, calmodulin (CaM). Calcium-bound CaM binds to the cytosolic IQ motif in the Sec61α subunit which leads to channel closure and prevents further calcium efflux.

undergo calcium signalling as known in higher eukaryotes, which eliminates the physiological need for translocon regulation dependent on Ca^{2+} influx and, (ii) accordingly, the IQ motif is conserved in higher eukaryotes but not in eubacteria or archaea (Table I). According to our model (Figure 7), the inactive ribosome–channel complex after termination of translocation as well as the ribosome-free translocon after ribosome dissociation allow for passive calcium efflux from the ER, which leads to the formation of a calcium nanodomain at the cytsolic channel mouth. After the binding of Ca^{2+} ions, activated CaM binds to the Sec61α IQ motif and induces channel closure, minimizing further calcium leakage and maintaining the important barrier at the ER membrane.

We expect that Ca^{2+} removal from calcium nanodomains as mediated by SERCA leads to dissociation of Ca^{2+} from CaM and, subsequently, reversal of the CaM effect on the Sec61 complex. This would start another round of Ca^{2+} release and Ca^{2+}-CaM-mediated conformational change in Sec61.

Remarkably, we also detected Ca^{2+}-independent binding of CaM to the purified, reconstituted Sec61 complex, which had no effect on channel closure but may preassociate apocalmodulin in proximity to the IQ motif. A comparable mechanism has been found for L- and P/Q-type Ca^{2+} channels (Zühlke *et al*, 1999; DeMaria *et al*, 2001). We suggest that binding of CaM to the IQ motif is Ca^{2+}-dependent and that there is a second Ca^{2+}-independent CaM-binding site present

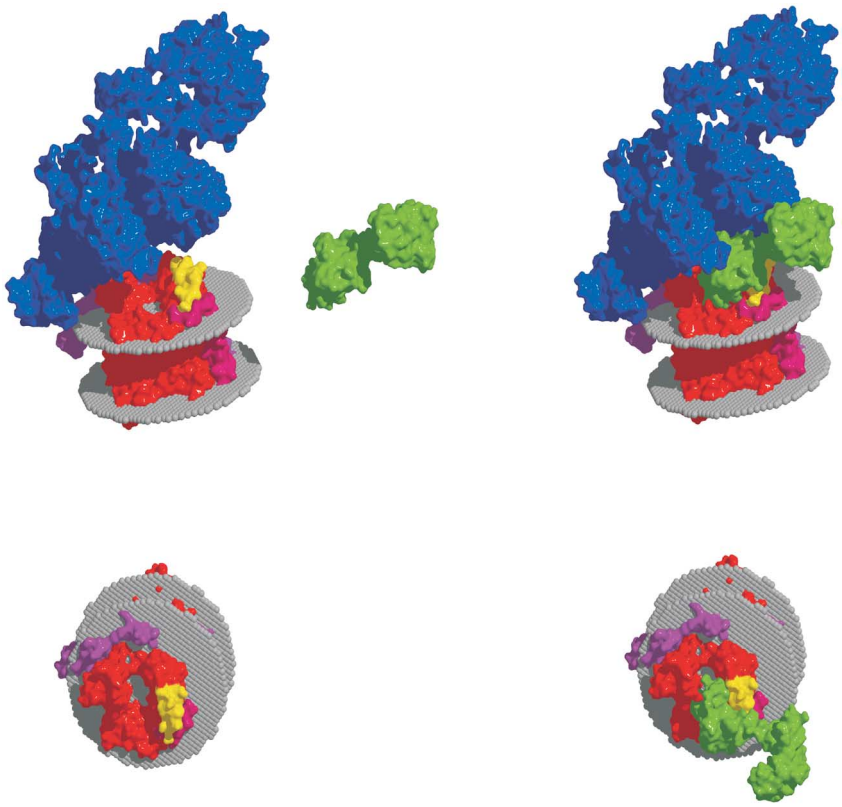

Figure 8 Molecular model for the ribosome/Sec61/CaM complex. We used the cryo-EM structure of the mammalian Sec61 complex (Sec61α, red; Sec61β, pink; Sec61γ, magenta) with the ribosome (blue). This structure has the pdb code 2wwb (Becker *et al*, 2009). First, calmodulin docking in the absence of the ribosome was performed using the docking program HEX (Ritchie *et al*, 2008). The crystal structure of calmodulin (green) with bound calcium ions was used (pdb 1CLL). The 50 best-scored binding modes were selected, and the structures that overlapped with the membrane and ribosome were deleted. The position of the membrane was predicted using the method of Lomize *et al* (2006) and is indicated as two planes of spheres. The resulting binding modes were found to be very similar to each other and showed the binding of the C-terminus of CaM to the IQ motif (yellow). According to this analysis, Ca^{2+}-CaM fills the gap between the ribosome and Sec61 complex without blocking the entrance to the polypeptide-conducting channel. We note that the N-terminus of CaM faces away from the ribosome and, therefore, N-terminal GST did not interfere in our experiments.

in the Sec61 complex. Indeed, bioinformatic analysis detected a potential CaM-binding site in Sec61γ that would reside in the cytosol (KPDRKEFQKIAMAT). In our gradient experiments, that is when free CaM was removed during flotation, this site was hardly detected and, therefore, CaM has lower affinity for this second site as compared to the IQ motif.

We propose that a CaM-mediated Ca^{2+}-based regulatory mechanism is operating for the protein translocase Sec61. This mechanism resembles the negative feedback regulation by Ca^{2+} known as calcium-dependent inactivation, which has been shown for various ion-conducting channels like NMDA receptors (Wang *et al*, 2008), as well as voltage-gated channels (Dick *et al*, 2008; Tadross *et al*, 2008).

We tested our hypothesis in a molecular modelling approach. Docking analysis revealed an almost perfect fit of Ca^{2+}-CaM into the gap between the Sec61 complex and ribosome (Figure 8; Supplementary Movies 1 and 2). Thus, molecular modelling of the ribosome/Sec61/CaM complex supports the idea that even the simultaneous binding of ribosomes and CaM to the Sec61 complex is possible.

Yet another potential level of regulation has to be considered. Dobberstein *et al* observed that, after cleavage from the respective precursor polypeptides by signal peptidase, signal peptides are typically split in half by signal peptide peptidase, and that N-terminal fragments from some signal peptides bind to CaM in a Ca^{2+}-dependent manner (Lyko *et al*, 1995). Therefore, a modulatory effect of these signal peptide fragments on the regulatory role of CaM in Ca^{2+} leakage from the ER would not be surprising.

Materials and methods

Materials

3-(3-Cholamidopropyl)dimethylammonio-1-propane sulfate, deoxy big CHAP, and CaM were purchased from Calbiochem and purified L-α phosphatidylcholine (egg) from Larodan Fine Chemicals. Trifluoperazine, fluoresceine, and anti-β-actin antibody were obtained from Sigma-Aldrich and Atto488 from Atto-Tec. The IQ peptide used for the FCS experiments was synthesized by GenScript Corp. FeBABE protein cutting reagent (Fe(III) (S)-1-(*p*-Bromoacetamidobenzyl)ethylenediamine tetraacetic acid) was obtained from Thermo Scientific. Enhanced chemiluminescence (ECL™), ECL™ Plex goat-anti-rabbit IgG-Cy5- and ECL™ Plex goat-anti-mouse IgG-Cy3-conjugate were purchased from GE Healthcare, thapsigargin and FURA-2-AM from invitrogen/molecular probes, and ophiobolin A and Nuclear-ID Blue/Green cell viability reagent from Enzo Life Sciences. The GST-CaM and GST (CaM from *Rattus rattus*, GST from *Schistosoma japonicum*) were purified as fusion proteins from *E. coli* according to standard procedures (Smith and Johnson,

1988). RM were prepared from dog pancreas (Dierks *et al*, 1996). Sec61 proteoliposomes were made from purified components as previously described (Wirth *et al*, 2003).

Fluorescence correlation spectroscopy

The following peptide sequence derived from the Sec61α subunit of *Canis lupus familiaris* [$_{16}$LPE$_{19}$IQKPERKIQFKEKV$_{32}$LWTAITLFI-C], which contains an additional terminal cysteine (1 mg) was labelled with Atto488maleimide dye and characterized as described in the methods section of Supplementary data in detail. FCS measurements were performed using an Insight Cell 3D laser scanning spectrometer (Evotech Technologies) as described in the methods section of Supplementary data. For the data analysis, a self-written software program (Alf Honigmann) was used. To obtain the K_D values, the resulting data points were fitted using the software Origin 7.0 (Microcal) according to a one site binding isotherm.

Peptide-spot binding assay

IQ peptides were synthesized on acid hardened cellulose membranes, derivatized with a polyethylene glycol spacer as described (Hilpert *et al*, 2007). Membranes were equilibrated in binding buffer (150 mM NaCl, 50 mM Tris/HCl (pH 7.5), 0.1% Triton X-100, and 1 mM $CaCl_2$ or 4 mM EGTA) for 2 h at 4°C. ^{14}C-labelled GST-CaM was added and incubated at 4°C overnight. The membrane was washed with binding buffer three times for 10 min each, dried at room temperature, and subjected to phosphorimaging using a Typhoon-Trio imaging device (GE Healthcare).

Sucrose gradient flotation

We incubated 10 μl of RM, PKRM, or Sec61 proteoliposomes (all corresponding to about 20 pmol heterotrimeric Sec61 complex) in 100 μl 150 mM KCl, 50 mM Hepes/KOH (pH 7.4), 5 mM $MgCl_2$, 10% sucrose, and 0.05 mg/ml BSA with 50 pmol GST-CaM and either 2 mM $CaCl_2$ or 4 mM EGTA for 60 min at 0°C. The samples were adjusted to 77% sucrose, 150 mM KCl, 50 mM Hepes/KOH (pH 7.4), 5 mM $MgCl_2$, and 0.05 mg/ml BSA (900 μl) and covered with a 62% (800 μl) and 8.5% (500 μl) sucrose cushion in 150 mM KCl, 50 mM Hepes/KOH (pH 7.4), 5 mM $MgCl_2$, 0.05 mg/ml BSA, and 2 mM $CaCl_2$ or 4 mM EGTA. The step gradients were centrifuged for 18 h at 116 000 × *g* in a SW55 rotor at 2°C and fractionated into 10 aliquots representing 12–70% sucrose densities. The protein content of the fractions was precipitated according to Wessel and Fluegge (1984). Samples were dissolved in SDS sample buffer, incubated for 10 min at 56°C, and analysed by SDS–PAGE and subsequent western blotting on PVDF membranes. Blots were incubated with antibodies against GST and Sec61β, respectively. Bound antibodies were visualized using peroxidase (POD)-coupled anti-rabbit antibodies and ECL^{TM} and detected with a Lumi-Imager F1 (Roche).

Single-channel recordings

Vesicles for planar bilayer experiments were prepared by mixing (3:2, v/v) the different Sec61-containing vesicles with preformed liposomes (egg L-α phosphatidylcholine, 10 mg/ml) in 50 mM KCl and 10 mM Mops/Tris (pH 7.0). Mega-9 (nonanoyl-*N*-methylglucamide) was added to a final concentration of 80 mM. After mixing, the sample was dialysed for 4 h at room temperature and then overnight at 4°C against a buffer (5 l) containing 50 mM KCl and 10 mM Mops/Tris (pH 7.0). Aliquots (10 μl, typically 10 mg/ml protein, lipid/protein 2:1 [w/w]) of the proteoliposomes derived from RM vesicles were incubated with 200 μM puromycin and 250–500 mM KCl for 15–30 min on ice.

Planar lipid bilayers were produced by the painting technique described previously (Müller *et al*, 1963). An osmotic gradient was used for vesicle fusion. Membrane potentials refer to the *trans* compartment. Data recording and analysis was performed as previously described (Wirth *et al*, 2003). Voltage ramps were conducted at a rate of 6.6 mV/s.

Cell culture

HeLa cells (ATCC no. CCL-2) were cultured at 37°C in Dulbecco's modified eagle medium (DMEM) medium (Gibco) containing 10% fetal bovine serum (Biochrom) and 1% penicillin/streptomycin (PAA) in a humidified environment with 5% CO_2. For live cell calcium imaging, cells were grown on 25 mm cover slips pretreated with poly-lysine (1 mg/ml) for 1 h.

Silencing of gene expression by siRNA

For gene silencing, 5.2×10^5 HeLa cells were seeded per 6 cm culture plate in normal culture. The cells were transfected with *SEC61A1* siRNA (GGAAUUUGCCUGCUAAUCAtt, Qiagen), *SEC61A1*-UTR siRNA (CACUGAAAUGUCUACGUUUtt, Qiagen), or control siRNA (AllStars Negative Control siRNA, Qiagen) using HiPerFect Reagent (Qiagen) according to the manufacturer's instructions (final concentration of siRNAs: 20 nM). After 24 h, the medium was changed and the cells were transfected a second time. Silencing was evaluated by western blot analysis using an antibody directed against the C-terminus of Sec61α protein and an anti-β-actin-antibody from mouse. The primary antibodies were visualized using ECL^{TM} Plex goat-anti-rabbit IgG-Cy5- or ECL^{TM} Plex goat-anti-mouse IgG-Cy3-conjugate and the Typhoon-Trio imaging system (GE Healthcare) in combination with the Image Quant TL software 7.0 (GE Healthcare). The maximum silencing effect was seen 96 h after the first transfection.

In order to rescue the phenotype of *SEC61A1* silencing, the *SEC61A1* cDNA was inserted into the multi-cloning site (MCS) of a pCDNA3-internal ribosomal entry site (IRES)-green fluorescent protein (GFP)-vector that contained the cytomegalovirus promoter, the MCS, the IRES, plus the GFP coding sequence. Cells were treated with *SEC61A1*-UTR siRNA as described above for 48 h. Subsequently, the cells were transfected with either vector or *SEC61A1* expression plasmids using Fugene HD (Roche). According to GFP fluorescence the transfection efficiency was around 80%.

Live cell calcium imaging

Live cell calcium imaging was carried out as previously described (Aneiros *et al*, 2005; Gross *et al*, 2009). HeLa cells were loaded with 4 μM FURA-2 AM in DMEM for 45 min at 25°C (Aneiros *et al*, 2005; Gross *et al*, 2009). Cells were washed twice and incubated in a calcium-free buffer (140 mM NaCl, 5 mM KCl, 1 mM $MgCl_2$, 0.5 mM EGTA, 10 mM glucose in 10 mM HEPES-KOH (pH 7.35)). During the experiment, cells were treated with one of the two CaM antagonists (10 μM trifluoperazine or 100 μM ophibolin A) or with the calcium-free buffer. After ratiometric measurements were carried out for 10 min, thapsigargin (1 μM) was added and the measurements continued. Where indicated, HeLa cells were treated with siRNA directed against *SEC61A1* or a negative control siRNA for 96 h prior to calcium imaging. Data were collected on an iMIC microscope and the polychromator V (Till Photonics) by alternately exciting at 340 and 380 nm and measuring the emitted fluorescence at 510 nm. Images containing 20–50 cells/frame were sampled every 3 s. FURA-2 signals were recorded as the ratios F340/F380, where F340 and F380 correspond to the background-subtracted fluorescence intensity at 340 and 380 nm, respectively. Cytoslic [Ca^{2+}] was estimated from ratio measurements by an established calibration method (Lomax *et al*, 2002). Data were analysed by Excel 2007 and Origin 6.1.

Protein transport experiments

Nascent preprolactin and mutant preprocecropin A were synthesized in reticulocyte lysate (Promega) in the presence of [^{35}S]methionine for 20 min at 30°C. The translation reaction contained EGTA at a concentration of ~400 μM. The translation reactions were divided into several aliquots, supplemented with RM as indicated, and incubated in the absence or presence of calcium (600–1200 μM) and CaM (60 μM) for 20 min at 30°C. The microsomes were re-isolated by centrifugation, re-suspended in cross-linking buffer (50 mM triethanolamine–HCl (pH 7.4), 200 mM sucrose, 50 mM KOAc, 5 mM MgOAc), and incubated an additional 20 min at 30°C in the absence or presence of puromycin (1.25 mM). Subsequently, the samples were subjected to treatment with protease or to chemical cross-linking. For protease treatment, samples were divided into two aliquots and incubated in the absence or presence of proteinase K (170 μg/ml) for 60 min at 0°C. Protease treatment was terminated by the addition of phenylmethylsulfonyl fluoride (10 mM). For cross-linking, samples were incubated with 335 μM succinimidyl 4-(*N*-maleimidomethyl)cyclohexane-1-carboxylate (SMCC; Pierce) for 30 min at 0°C. All samples were subjected to SDS–PAGE and phosphorimaging in the Typhoon-Trio imaging system.

Supplementary data

Supplementary data are available at *The EMBO Journal* Online (http://www.embojournal.org).

Acknowledgements

We are grateful to Drs Ulrich Wissenbach and Veit Flockerzi (both Homburg) for supplying the pCDNA3-IRES-GFP vector. We acknowledge the technical assistance from Simone Amann, Ulrike Klemstein, Monika Lerner, Heidi Löhr, Anika Müller (all Homburg), and Birgit Hemmis (Osnabrück). We thank Dr Stefan Walter (Osnabrück) for his help with the mass spectrometry experiments. This interdisciplinary work would not have been possible without various Deutsche Forschungsgemeinschaft-funded coordinated research programs (FOR 967, GRK 845, GRK 1276/1, GRK 1326, SFB 530).

Conflict of interest

The authors declare that they have no conflict of interest.

References

Alder NN, Shen Y, Brodsky JL, Hendershot LM, Johnson AE (2005) The molecular mechanisms underlying BiP-mediated gating of the Sec61 translocon of the endoplasmic reticulum. *J Cell Biol* **168:** 389–399

Allbritton NL, Meyer T, Stryer L (1992) Range of messenger action of calcium ion and inositol 1,4,5-trisphosphate. *Science* **258:** 1812–1815

Alvarez J (2002) Measuring [Ca2 +] in the endoplasmic reticulum with aequorin. *Cell Calcium* **32:** 251–260

Aneiros E, Philipp SE, Lis A, Freichel M, Cavalie A (2005) Modulation of Ca2 + signalling by Na + /Ca2 + exchangers in mast cells. *J Immunol* **174:** 119–130

Au TK, Chick WS, Leung PC (2000) The biology of ophiobolins. *Life Sci* **67:** 733–742

Babu YS, Sack JS, Greenhough TJ, Bugg CE, Means AR, Cook WJ (1985) Three-dimensional structure of calmodulin. *Nature* **315:** 37–40

Bähler M, Rhoads A (2002) Calmodulin signaling via the IQ motif. *FEBS Lett* **513:** 107–113

Becker T, Bhushan S, Jarasch A, Armache JP, Funedad S, Jossinet F, Gumbart J, Mielke T, Berninghausen O, Schulten K, Westhof E, Gilmore R, Mandon ES, Beckmann R (2009) Structure of monomeric yeast and mammalian Sec61 complexes interacting with the translating ribosome. *Science* **326:** 1369–1373

Berridge MJ (2002) The endoplasmic reticulum: a multifunctional signalling organelle. *Cell Calcium* **32:** 235–249

Blobel G, Dobberstein B (1975) Transfer of proteins across membranes. I. Presence of proteolytically processed and unprocessed nascent immunoglobulin light chains on membrane-bound ribosomes of murine myeloma. *J Cell Biol* **67:** 835–851

Boehning D, Joseph SK, Mak DO, Foskett JK (2001) Single-channel recordings of recombinant inositol trisphosphate receptors in mammalian nuclear envelope. *Biophys J* **81:** 117–124

Camello C, Lomax R, Petersen OH (2002) Calcium leak from intracellular stores-the enigma of calcium signalling. *Cell Calcium* **32:** 355–361

Crowley KS, Liao S, Worrell VE, Reinhart GD, Johnson AE (1994) Secretory proteins move through the endoplasmic reticulum membrane via an aqueous, gated pore. *Cell* **78:** 461–471

DeMaria CD, Soong TW, Alseikhan BA, Alvania RS, Yue DT (2001) Calmodulin bifurcates the local Ca2 + signal that modulates P/Q-type Ca2 + channels. *Nature* **411:** 484–489

Dick IE, Tadross MR, Liang H, Tay LH, Yang W, Yue DT (2008) A modular switch for spatial Ca2 + selectivity in the calmodulin regulation of CaV channels. *Nature* **451:** 830–834

Dierks T, Volkmer J, Schlenstedt G, Jung C, Sandholzer U, Zachmann K, Schlotterhose P, Neifer K, Schmidt B, Zimmermann R (1996) A microsomal ATP-binding protein involved in efficient protein transport into the mammalian endoplasmic reticulum. *EMBO J* **15:** 6931–6942

Erdmann F, Jung M, Eyrisch S, Lang S, Helms V, Wagner R, Zimmermann R (2009) Lanthanum inhibits the mammalian Sec61 complex in its channel dynamics and protein transport activity. *FEBS Lett* **583:** 2359–2364

Flourakis M, Van Coppenolle F, Lehen'kyi V, Beck B, Skryma R (2006) Passive calcium leak via translocon is a first step for iPLA2-pathway regulated store operated channels activation. *FASEB J* **20:** 1215–1217

Foskett JK, White C, Cheung KH, Mak DO (2007) Inositol trisphosphate receptor Ca2 + release channels. *Physiol Rev* **87:** 593–658

Ghaim JB, Greiner DP, Meares CF, Gennis RB (1995) Proximity mapping the surface of a membrane protein using an artificial protease: demonstration that the quinone-binding domain of subunit I is near the N-terminal region of subunit II of cytochrome bd. *Biochemistry* **34:** 10311–10315

Giunti R, Gamberucci A, Fulceri R, Banhegyi G (2007) Both translocon and a cation channel are involved in the passive Ca2 + leak from the endoplasmic reticulum: a mechanistic study on rat liver microsomes. *Arch Biochem Biophys* **462:** 115–121

Görlich D, Rapoport TA (1993) Protein translocation into proteoliposomes reconstituted from purified components of the endoplasmic reticulum membrane. *Cell* **75:** 615–630

Gross SA, Guzman GA, Wissenbach U, Philipp SE, Zhu MX, Bruns D, Cavalie A (2009) TRPC5 is a Ca2 + -activated channel functionally coupled to Ca2 + -selective ion channels. *J Biol Chem* **284:** 34423–34432

Hamman BD, Chen JC, Johnson AE (1997) The aqueous pore through the translocon has a diameter of 40–60 A during cotranslational protein translocation at the ER membrane. *Cell* **89:** 535–544

Hamman BD, Hendershot LM, Johnson AE (1998) BiP maintains the permeability barrier of the ER membrane by sealing the lumenal end of the translocon pore before and early in translocation. *Cell* **92:** 747–758

Hartmann E, Sommer T, Prehn S, Gorlich D, Jentsch S, Rapoport TA (1994) Evolutionary conservation of components of the protein translocation complex. *Nature* **367:** 654–657

Hilpert K, Winkler DF, Hancock RE (2007) Peptide arrays on cellulose support: SPOT synthesis, a time and cost efficient method for synthesis of large numbers of peptides in a parallel and addressable fashion. *Nat Protoc* **2:** 1333–1349

Johnson JD, Fugman DA (1983) Calcium and calmodulin antagonists binding to calmodulin and relaxation of coronary segments. *J Pharmacol Exp Ther* **226:** 330–334

Leung PC, Tylor WA, Wang JH, Tipton CL (1984) Ohpiobolin A. A natural product inhibitor of calmodulin. *J Biol Chem* **259:** 2742–2747

Lomax RB, Camello C, Van Coppenolle F, Petersen OH (2002) Basal and physiological Ca2 + leak from the endoplasmic reticulum of pancreatic acinar cells. Second messenger-activated channels and translocons. *J Biol Chem* **277:** 26479–26485

Lomize AL, Pogozheva ID, Lomize MA, Mosberg HI (2006) Positioning of proteins in membranes: a computational approach. *Prot Sci* **15:** 1318–1333

Lyko F, Martoglio B, Jungnickel B, Rapoport TA, Dobberstein B (1995) Signal sequence processing in rough microsomes. *J Biol Chem* **270:** 19873–19878

Menetret J-F, Hegde RS, Aguiar M, Gygi SP, Park E, Rapoport TA, Akey CW (2008) Single copies of Sec61 and TRAP associate with a nontranslating mammalian ribosome. *Structure* **16:** 1126–1137

Müller P, Rudin D, Tien R, Westcott WC (1963) Methods for the formation of single bimolecular lipid membranes in aqueous solution. *J Phys Chem* **67:** 534–535

Ong HL, Liu X, Sharma A, Hegde RS, Ambudkar IS (2007) Intracellular Ca2 + release via the ER translocon activates store-operated calcium entry. *Pflugers Arch* **453:** 797–808

Petrasek Z, Schwille P (2008) Precise measurement of diffusion coefficients using scanning fluorescence correlation spectroscopy. *Biophys J* **94:** 1437–1448

Potter MD, Nicchitta CV (2002) Endoplasmic reticulum-bound ribosomes reside in stable association with the translocon following termination of protein synthesis. *J Biol Chem* **277:** 23314–23320

Puntervoll P, Linding R, Gemund C, Chabanis-Davidson S, Mattingsdal M, Cameron S, Martin DM, Ausiello G, Brannetti B, Costantini A, Ferrè F, Maselli V, Via A, Cesareni G, Diella F,

Superti-Furga G, Wyrwicz L, Ramu C, McGuigan C, Gudavalli R *et al* (2003) ELM server: a new resource for investigating short functional sites in modular eukaryotic proteins. *Nucleic Acids Res* **31:** 3625–3630

Rhoads AR, Friedberg F (1997) Sequence motifs for calmodulin recognition. *FASEB J* **11:** 331–340

Ritchie DW, Kozakov D, Vajda S (2008) Accelerating and focusing protein-protein docking correlations using multi-dimensional rotational FFT generating functions. *Bioinformatics* **24:** 1865–1873

Rizzuto R, Pozzan T (2006) Microdomains of intracellular Ca2 + : molecular determinants and functional consequences. *Physiol Rev* **86:** 369–408

Roy A, Wonderlin WF (2003) The permeability of the endoplasmic reticulum is dynamically coupled to protein synthesis. *J Biol Chem* **278:** 4397–4403

Saparov SM, Erlandson K, Cannon K, Schaletzky J, Schulman S, Rapoport TA, Pohl P (2007) Determining the conductance of the SecY protein translocation channel for small molecules. *Mol Cell* **26:** 501–509

Schaletzky J, Rapoport TA (2006) Ribosome binding to and dissociation from translocation sites of the ER membrane. *Mol Biol Cell* **17:** 3860–3869

Simon SM, Blobel G (1991) A protein-conducting channel in the endoplasmic reticulum. *Cell* **65:** 371–380

Smith AJ, Surviladze Z, Gaudet EA, Backer JM, Mitchell CA, Wilson BS (2001) p110beta and p110delta phosphatidylinositol 3-kinases up-regulate Fc(epsilon)RI-activated Ca2 + influx by enhancing inositol 1,4,5-trisphosphate production. *J Biol Chem* **276:** 17213–17220

Smith DB, Johnson KS (1988) Single-step purification of polypeptides expressed in Escherichia coli as fusions with glutathione S-transferase. *Gene* **67:** 31–40

Tadross MR, Dick IE, Yue DT (2008) Mechanism of local and global Ca2 + sensing by calmodulin in complex with a Ca2 + channel. *Cell* **133:** 1228–1240

Van Coppenolle F, Vanden Abeele F, Slomianny C, Flourakis M, Hesketh J, Dewailly E, Prevarskaya N (2004) Ribosome-translocon complex mediates calcium leakage from endoplasmic reticulum stores. *J Cell Sci* **117:** 4135–4142

Van den Berg B, Clemons J, Collinson I, Modis Y, Hartmann E, Harrison SC, Rapoport TA (2004) X-ray structure of a protein-conducting channel. *Nature* **427:** 36–44

Vandonselaar M, Hickie RA, Quail JW, Delbaere LTJ (1994) Trifuoperazine-induced conformational change in Ca2 + -calmodulin. *Nat Struct Biol* **1:** 795–801

Wang C, Wang HG, Xie H, Pitt GS (2008) Ca2 + /CaM controls Ca2 + -dependent inactivation of NMDA receptors by dimerizing the NR1 C termini. *J Neurosci* **28:** 1865–1870

Wessel D, Fluegge UI (1984) A method for the quantitative recovery of protein in dilute solution in the presence of detergent and lipids. *Anal Biochem* **138:** 141–143

Wirth A, Jung M, Bies C, Frien M, Tyedmers J, Zimmermann R, Wagner R (2003) The Sec61p complex is a dynamic precursor activated channel. *Mol Cell* **12:** 261–268

Wonderlin WF (2009) Constitutive, translation-independent opening of the protein-conducting channel in the endoplasmic reticulum. *Pflugers Arch* **457:** 917–930

Wuytack F, Raeymaekers L, Missiaen L (2002) Molecular physiology of the SERCA and SPCA pumps. *Cell Calcium* **32:** 279–305

Xu L, Mann G, Meissner G (1996) Regulation of cardiac Ca2 + release channel (ryanodine receptor) by Ca2 + , H + , Mg2 + , and adenine nucleotides under normal and simulated ischemic conditions. *Circ Res* **79:** 1100–1109

Yamada M, Miyawaki A, Saito K, Nakajima T, Yamamoto-Hino M, Ryo Y, Furuichi T, Mikoshiba K (1995) The calmodulin-binding domain in the mouse type 1 inositol 1,4,5-trisphosphate receptor. *Biochem J* **308:** 83–88

Yamaguchi N, Xin C, Meissner G (2001) Identification of apocalmodulin and Ca2 + -calmodulin regulatory domain in skeletal muscle Ca2 + release channel, ryanodine receptor. *J Biol Chem* **276:** 22579–22585

Yap KL, Kim J, Truong K, Sherman M, Yuan T (2000) Calmodulin target database. *J Struct Funct Genomics* **1:** 8–14

Yu R, Hinkle PM (2000) Rapid turnover of calcium in the endoplasmic reticulum during signalling. Studies with cameleon calcium indicators. *J Biol Chem* **275:** 23648–23653

Zühlke RD, Pitt GS, Deisseroth K, Tsien RW, Reuter H (1999) Calmodulin supports both inactivation and facilitation of L-type calcium channels. *Nature* **399:** 159–162